

FUNCTIONAL GRADIENT MATERIAL OF Ti-6Al-4V AND γ -TiAl FABRICATED BY ELECTRON BEAM SELECTIVE MELTING

Wenjun Ge*†, Feng Lin*†, Chao Guo*†

*Key Laboratory for Advanced Materials Processing Technology, Ministry of Education of China, Tsinghua University, Beijing 100084, P.R. China

†Center for Bio-manufacturing and Rapid Forming Technology, Department of Mechanical Engineering, Tsinghua University, Beijing 100084, P.R. China

REVIEWED

Abstract

Additive Manufacturing (AM) technologies are very promising in fabricating functionally graded materials. Electron Beam Selective Manufacturing (EBSM) is one widely used AM technology capable of fabricating a variety of materials especially titanium alloys. Previous studies on EBSM process were focused on the manufacturing of one single material. In this study, a novel EBSM process capable of building gradient structures with dual metal materials was developed. Ti6Al4V powders and Ti47Al2Cr2Nb powders were used to fabricate Ti₃Al/TiAl and Ti6Al4V/Ti₃Al dual metal structures. The chemical compositions, microstructure and micro-hardness of the dual material samples were investigated employing Optical Microscope (OM), Scanning Electronic Microscope (SEM), Electron Probe Micro-Analyzer (EPMA). Results showed that the thickness of the transition zone was about 300 μ m. The transition zone was free of cracks, and the chemical compositions exhibited a staircase-like change. The microstructure and chemical compositions in different regions were studied. Micro-hardness was affected by the microstructure. The microstructures turned out to be full lamellar at the TiAl region and basket-weave structure at the Ti₃Al and Ti6Al4V region.

Introduction

Titanium (Ti) alloys are widely used in the aerospace and aviation industries because of their excellent properties including low density, high specific strength, excellent corrosion resistance in various kinds of environment and good high-temperature performances. Ti6Al4V have been widely studied but the working temperature is relatively low. Both the TiAl and Ti₃Al-based alloys are attractive materials for high temperature structural applications in aerospace industry due to their high specific strength and good oxidation resistance at elevated temperature [1~4]. However, they suffer from poor ductility at the room temperature and low fracture toughness, which prevent their commercial exploitation [4].

Functional Gradient Material (FGM) shows great potentials for the applications in aerospace, dynamic high-pressure technology and medical implants [5]. Specifically, in the aerospace industry, compressors and turbine disks, which are no doubt the most significant parts, require different material properties at different regions. For instance, the rim regions, which suffer from high temperature and relatively small centrifugal force, mainly require good oxidation resistance. On the other hand, the core regions are faced with challenges of extremely

large centrifugal force and relatively low temperature, and require high strength rather than good oxidation resistance. Yang [6] reported that the rim of a dual alloy disk can be made of intermetallic such as Ti_3Al or $TiAl$ alloy with good high-temperature properties, and the core can be made of titanium alloy such as TC4 or TC11 with good properties at relatively low temperatures.

Additive Manufacturing (AM) technologies are quite promising in the fabrications of FGM. Most of the current additively manufactured FGMs were fabricated by laser-based additive manufacturing technologies e.g. Selective Laser Melting (SLM). Xiehang [7] fabricated the $Ti6Al4V-CoCrMo$ thin wall gradient material through laser direct forming and investigated the effect of $CoCrMo$ volume fraction on the cracking behaviors. The main reasons of the fracture are that the limited solid solution network $CoCrMo$ caused the stress concentration and the mismatch of thermal properties. Xi [8] investigated laser rapid forming of 316L stainless steel/ Ni -based alloy/ $Ti6Al4V$ gradient materials. The phase change in the gradient segment of Ni -based alloy and $Ti6Al4V$ was studied and they found that the hardness values decreased with the increase of the content of $Ti6Al4V$. Xu [9] fabricated $TC11/\gamma-TiAl$ bio-materials using laser deposition process. According to his study, the compositions insignificantly affected the cracks in the transition zone. The microstructure transformation mechanisms of $TiAl$ and TC4 were also investigated. Douglas C. Hofmann [10] fabricated $Ti6Al4V-V$ gradient metal alloys through laser-based radial deposition additive manufacturing.

However, one main problem of the laser-based AM technologies is the fracture and the oxidation. Electron Beam Selective Melting (EBSM) has several advantages over laser-based AM technologies in functional gradient titanium alloys. First, preheating the base plate and the powder bed to a high temperature could reduce the thermal stress, especially for the brittle materials like $TiAl$ and Ti_3Al . In addition, the vacuum environment could prevent the introduction of impurity elements. In this work, we fabricated FGMs employing a novel EBSM system developed by Tsinghua University. $TiAl/Ti_3Al$ and $Ti6Al4V/Ti_3Al$ FGMs were designed and fabricated. The Ti_3Al was obtained by mixing the two metal powders of $TiAl$ and $Ti6Al4V$. The two powders can form homogenous chemical compositions in the melting process. The chemical compositions, microstructure and micro-hardness were studied.

Material and experiment procedure

Two kinds of titanium alloy FGMs were fabricated through EBSM. The EBSM system used in this study was developed by the Center for Bio-manufacturing and Rapid Forming Technology in the Department of Mechanical Engineering, Tsinghua University. Figure.1 shows the schematics of the supplying system of dual powders [11]. This system contains vibrator, two powder tanks and powder-mixing box. Once the value of two powders has been set, the vibrators vibrate to make the powder flow and dropped into the powder-mixing box precisely and then the powder-mixing box rotates back and forth several times to make the composition homogenous. Finally, the mixed powders were spread onto the base plate.

Atomized $Ti6Al4V$ and $Ti47Al2Cr2Nb$ powders were used to fabricate $Ti6Al4V/Ti_3Al$ and $TiAl/Ti_3Al$ gradient materials. Ti_3Al was obtained through the mixing of $Ti6Al4V$ and $Ti47Al2Cr2Nb$. Figure.2 schematically shows the two samples.

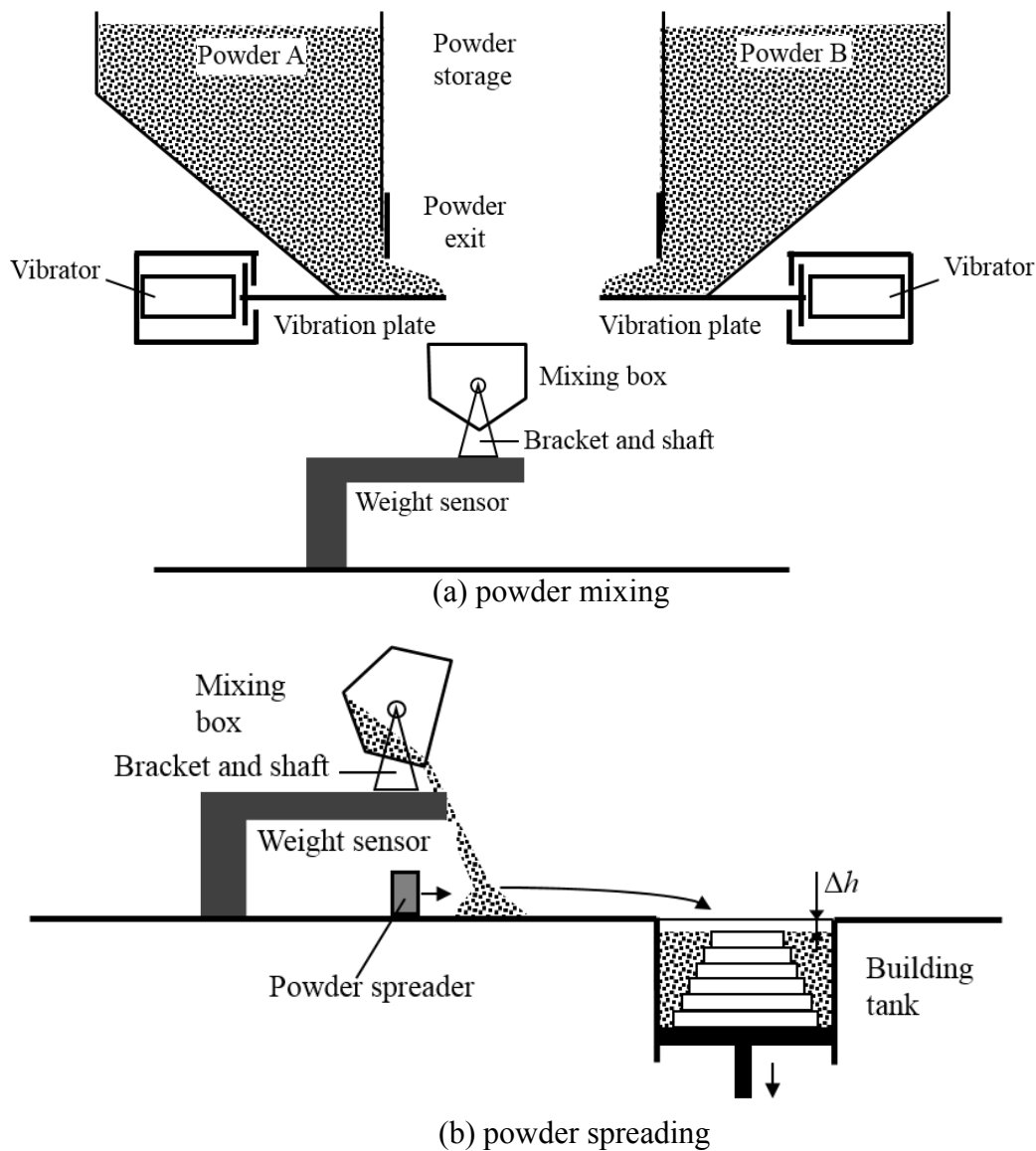


Figure.1 Powder supplying system

The baseboard of 316L stainless steel with the dimensions of 90mm× 90mm×10mm, was grounded and washed in ethanol to remove surface oxidation film, before it was placed into the vacuum chamber. The substrate was firstly preheated to 800°C using a defocused electron beam. Besides, during the fabrication process, each 100μm thick layer of blended powders was also preheated to be lightly sintered employing the beam current ranging from 1mA to 15mA and the scanning velocity of 5m/s. For each layer, the compositions are affected by both the fabrication parameters and the compositions of the following deposited layers. In order to investigate the effects of the fabrication parameters on the transition zone, the samples were fabricated with different beam currents as shown in Table.1 (wt% denotes the mass percentage). For example, every layer of Sample-1 was scanned to be melted for 3 times with the increasing beam currents from 4mA to 8mA, and then to 12mA. Then a new layer of powders was spread on top of the

previous layer, and the preheating and melting process were repeated until the sample was finished.

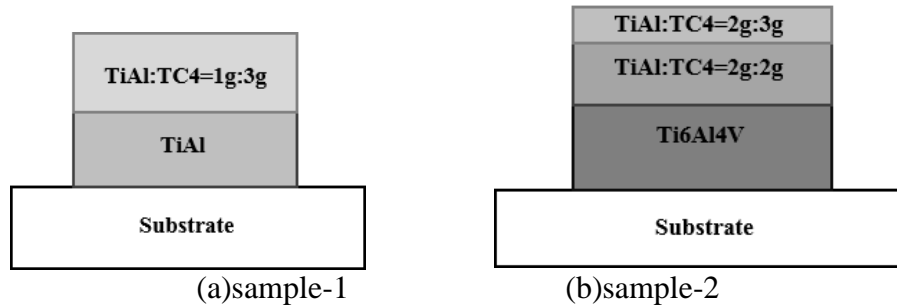


Figure.2 Composition model of dual metal materials

The samples were cut along the building direction using Wire Electrical Discharge Machining and then mounted, ground, polished and etched utilizing Kroll's reagent (2% HF, 5% HNO₃ and 93% H₂O). Micro-hardness was measured on MH-3 microhardness tester with the load of 200g and the dwelling time of 15s. Microstructures of EBSM fabricated components were observed via Optical Microscope (OM) and Scanning Electron Microscope (SEM). Semi-quantitative and quantitative analyses of the chemical compositions were performed using Electron Probe Micro-Analyzer (EPMA).

Table.1 Compositions and fabrication parameters of each layer

	Layer	wt% TC4	wt% TiAl	Beam Current	Scanning speed
Sample-1	0-10	0%	100%	2mA-6mA	0.2m/s
	10-20	50%	50%	4mA-8mA-12mA	0.5m/s
Sample-2	0-30	100%	0%	2mA-4mA-6mA	0.5m/s
	30-45	50%	50%	2mA-4mA-6mA	0.5m/s
	45-50	40%	60%	2mA-4mA-6mA	0.5m/s

Results

Chemical compositions

To avoid the delamination, the previously formed layer needs to be at least partially re-melted. The re-melting depth would also significantly affect the composition gradient of the transition zone. Therefore, the compositions of the transition zone could be significantly affected by the fabrication parameters such as electron beam current, scanning speed and layer thickness. Semi-quantitative and quantitative analyses of the as-built samples were performed employing EPMA. Figure.3 shows the top region of the transition zone of Sample-1. As shown in Figure.3, there were no cracks or un-melted powders and the chemical compositions were relatively uniform in the transition zone. There were two zones with different chemical compositions and both the heights were 100um which is the same with the layer thickness. The compositions of the

transition zone varied stepwise, due to the layer-fashioned manufacturing process. EPMA analysis results showed that element change in the transition gradient zone. When the first layer of Ti_3Al was deposited on top of the Ti_6Al_4V or $TiAl$, a portion of Ti_6Al_4V or $TiAl$ was re-melted and mixed with the melted powders of Ti_3Al in the molten pool. According to the distribution of elementary Al and Ti, the re-melting depth of $TiAl$ could be calculated to be about $200\mu m$.

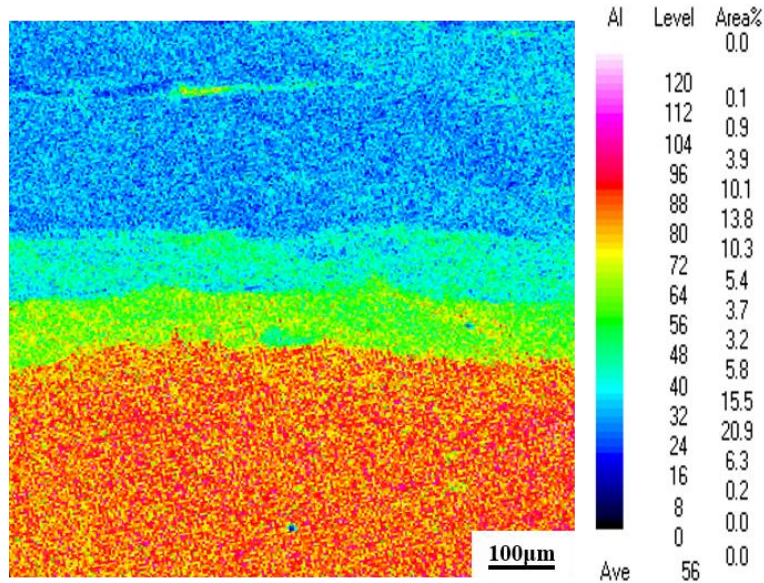
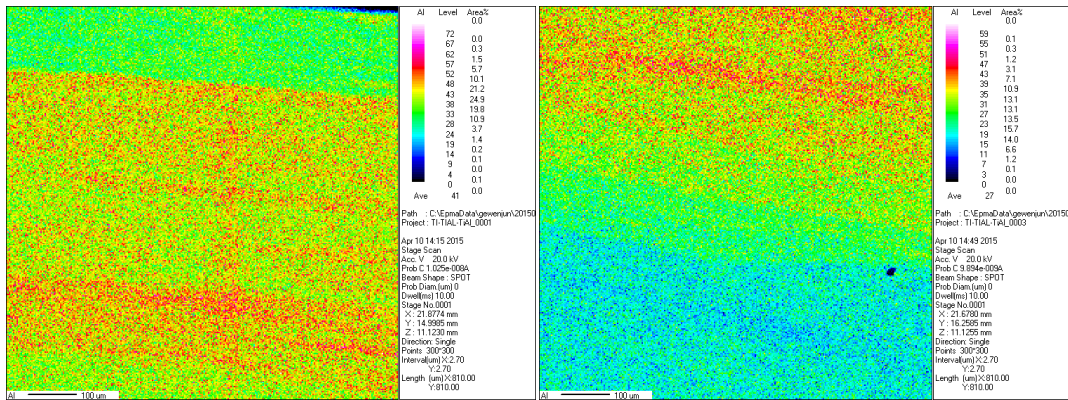


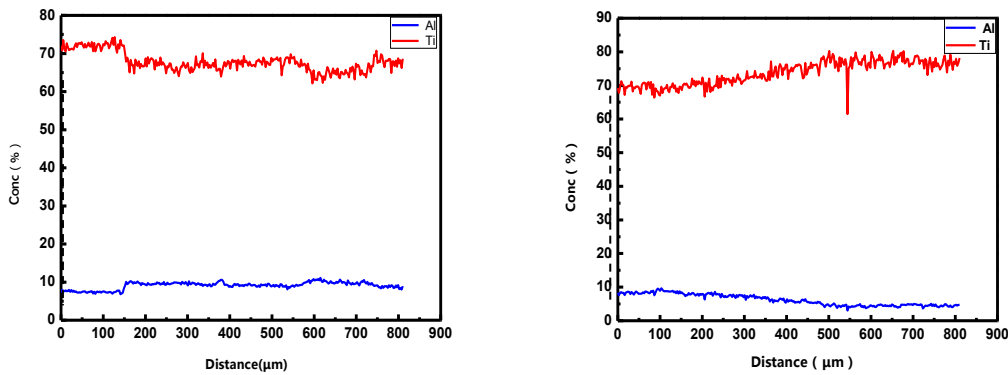
Figure.3 Chemical composition of transition region of Sample-1

For the $Ti_6Al_4V-Ti_3Al$ sample, there are two transition regions. Figure.4 shows the surface scan results of the top and middle transition regions. The results indicated that the top layer as the final deposition layer had a depth of $180\mu m$. Considering that the powder layer was $100\mu m$ thick, it can be concluded that the height of the re-melted layer thickness was $80\mu m$. The results of the line scan showed the distribution of elementary Al and Ti in the transition zone as Figure.5. The depth of the middle transition zone was $400\mu m$ and the content of Ti and Al changed gradually. In the top transition region, the curve is flatter except the top layer. Compared with the $Ti_3Al-TiAl$ gradient zone, composition changed more smoothly in the $Ti_3Al-Ti_6Al_4V$ transition zone. No step shapes could be seen on the curve. The reason is that the composition difference between Ti_3Al and Ti_6Al_4V is lower than the difference between $TiAl$ and Ti_3Al . Also, the re-melting depth h is smaller resulting in a smooth change.



(a) top transition region (b) middle transition region

Figure.4 Surface scan results



(a) top transition region (b) middle transition region

Figure.5 Liner scanning results

Microstructure evolutions

The properties of gamma TiAl alloys depend strongly on the grain size and the thickness of γ -TiAl and α_2 -Ti₃Al lamellar. Refined full lamellar microstructures are most attractive, since they offer controllable strengths, good creep and fatigue resistance, good fracture toughness and reasonable room temperature ductility. As can be seen in Figure.6 (d), the microstructure of TiAl part was full γ -TiAl and α_2 -Ti₃Al lamellar. The size of the lamellar cluster was 15~30 μm , which is finer than as-cast TiAl alloy full lamellar microstructure(200 μm).As in the as-built sample, a refined lamellar colony of 15 μm in size was found along the whole TiAl part.

In the Ti₃Al region, EPMA quantitative analysis results showed that Al content was 26wt.%. According to Ti-Al phase diagram [12], α phase transformed to α_2 phase. The phases at Ti₃Al region consist of α_2 , β /B2 forming basket-weave structure. Figure.6 (b) and (c) show the microstructure of transition zone and the top zone. It can be observed that in the transition zone the width and length of α_2 are 0.5 μm and 5 μm respectively, while in the top zone the width and length are 1 μm and 10 μm respectively.

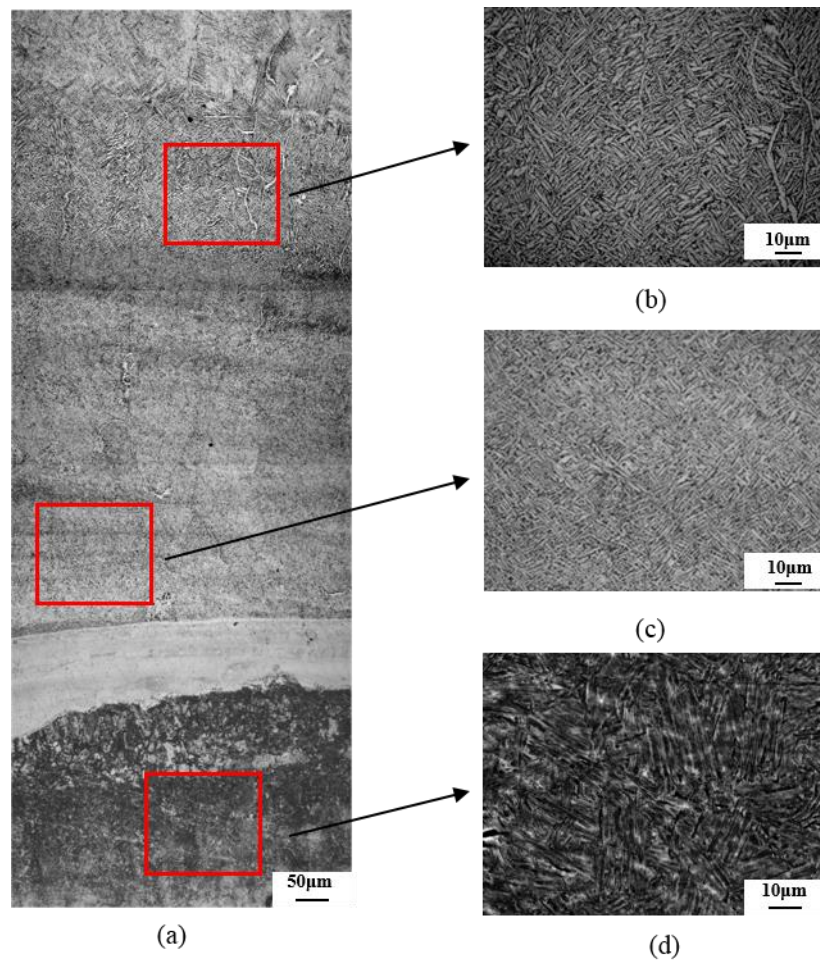


Figure.6 microstructures of sample-1

Figure.7 shows the OM images and SEM images of Sample-2. The images show that the microstructures of Ti6Al4V part are of typical EBSM fabrication features. Microstructures of EBSM produced Ti6Al4V alloy consist of large columnar prior β grains (see Figure.7(c)) growing along the building direction and basket-weave ($\alpha+\beta$) structure and Widmanstätten α platelets (see Figure.7(d)). The width of prior columnar β grains was about 100 μm . Fine α platelets are precipitated along the β grain boundary and inside the grains. It should be noted that the average α platelets thickness was 2 μm forming basket-weave and Widmanstätten structure.

The microstructures of Ti₃Al part can be seen in Fig.7 (a) and (b). It can be observed that the α_2 phase exhibits long lath-like shapes on the top region in Fig.7 (a) while it exhibits short-rod-like shapes in Fig.7 (b) in the middle region. The thickness of α_2 -laths was 1 μm which was finer than Ti6Al4V region.

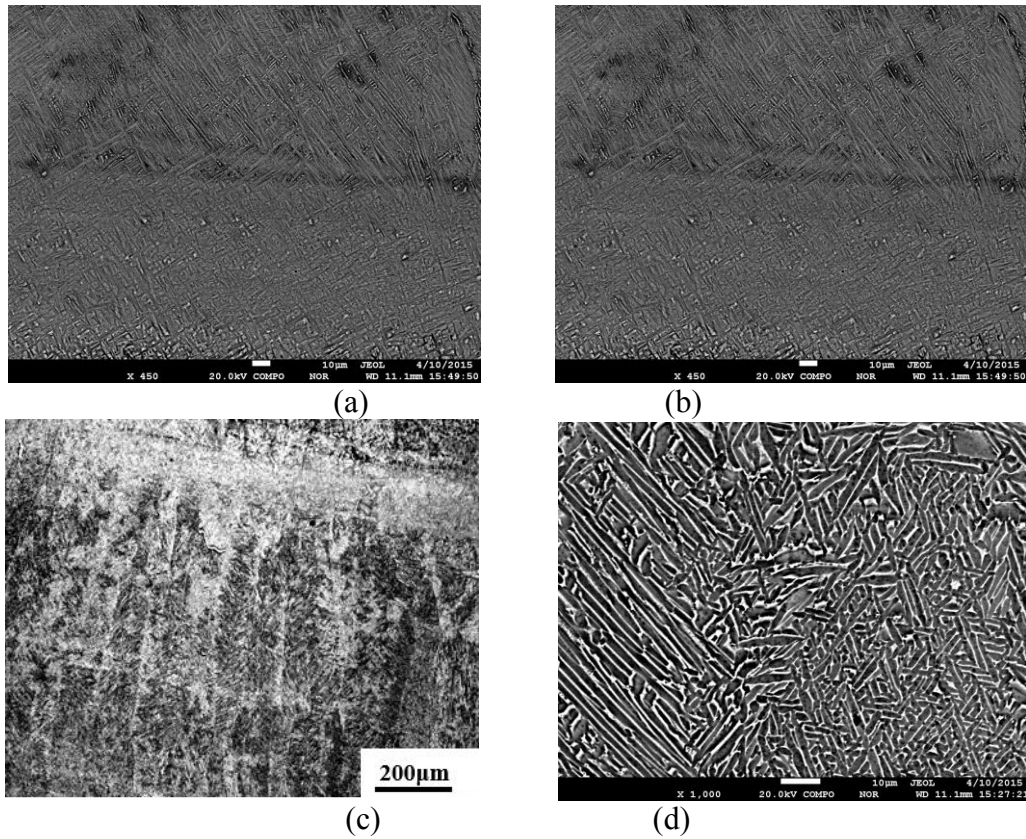


Figure.7 Microstructures of Sample-2

Micro-hardness

Figure.8 shows the Vickers micro-hardness of the dual alloy specimens measured from Ti_3Al region to $TiAl$ region. Since the deposition layer thickness was $100\mu m$, the interval between measuring points was $50\mu m$. From the result, it can be observed that from the Ti_3Al region to $TiAl$ region the fluctuations are small. Its maximum value is up to $450MPa$ at the Ti_3Al region. The first two points represent the top region of Ti_3Al and the micro-hardness is higher than the bottom region of Ti_3Al . The reason is that the microstructure at the top region is fine martensitic α laths. In the transition zone, the hardness shows a normal level distributing in the range of $350MPa-400MPa$.

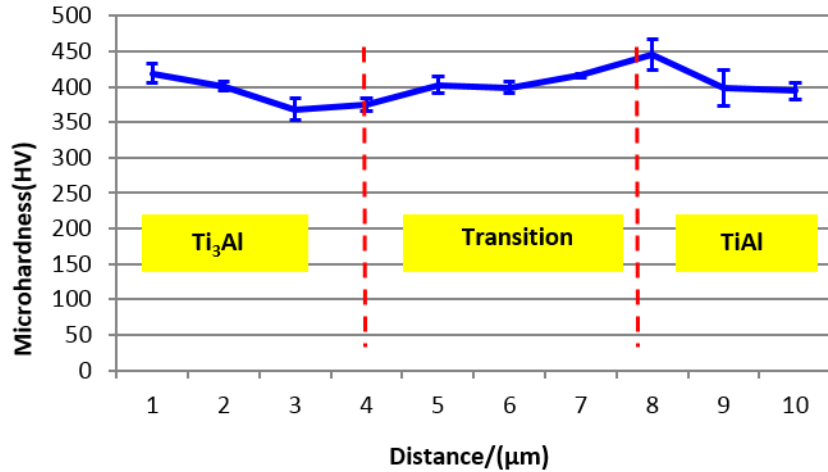


Figure.7 Micro-hardness along the building direction of sample-1

Discussion

The previously fabricated layer needs to be melted and that will make a dilution in composition. The penetration depth was significantly affected by the process parameters such as electron beam current, scanning speed and layer thickness. Based on the re-melting depth the composition change can be calculated.

The following simplifying assumptions could be made.

- (1) In the deposition layer, composition is homogenous.
- (2) The solid diffusion of element is ignored. The composition of forming layers will not change.
- (3) The shrinkage of the powder layer after melting is ignored. Shrinkage of the melting layer affect the height The height of the melting layer is fixed according to different parameters.

The formula:

ρ density change:

$$\rho_0 = \frac{\rho_{Ti-1}h + \rho_{Ti-2}H}{h+H} \quad (1)$$

$$\rho_n = \frac{\rho_{n-1}h + \rho_{Ti-2}H}{h+H} \quad (2)$$

h : depth of re-melting base material

H : deposition layer thickness

ρ_0 : density of first mixing layer

ρ_n : density of layer n

ρ_{Ti-1} : density of titanium alloy 1

ρ_{Ti-2} : density of titanium alloy 2

Percentage of element Al change:

$$\alpha_0 = \frac{\rho_{Ti-1}hf_1 + \rho_{Ti-2}f_2}{\rho_{Ti-1}h + \rho_{Ti-2}H} \quad (3)$$

$$a_n = \frac{\rho_n h a_{n-1} + \rho_{Ti-2} f_2}{\rho_n h + \rho_{Ti-2} H} \quad (4)$$

a_0 : mass fraction of element Al of first layer

a_n : mass fraction of element Al of layer n

f_1 : mass fraction of element Al of alloy 1

f_2 : mass fraction of element Al of alloy 2

The theoretical calculation and measured results of the elementary distribution is shown in Figure.8. From the result, it can be conclude that the result of tested is well matched the calculation. This validated theoretical model is able to provide both accurate explanations and design disciplines for the fabrications of FGMs.

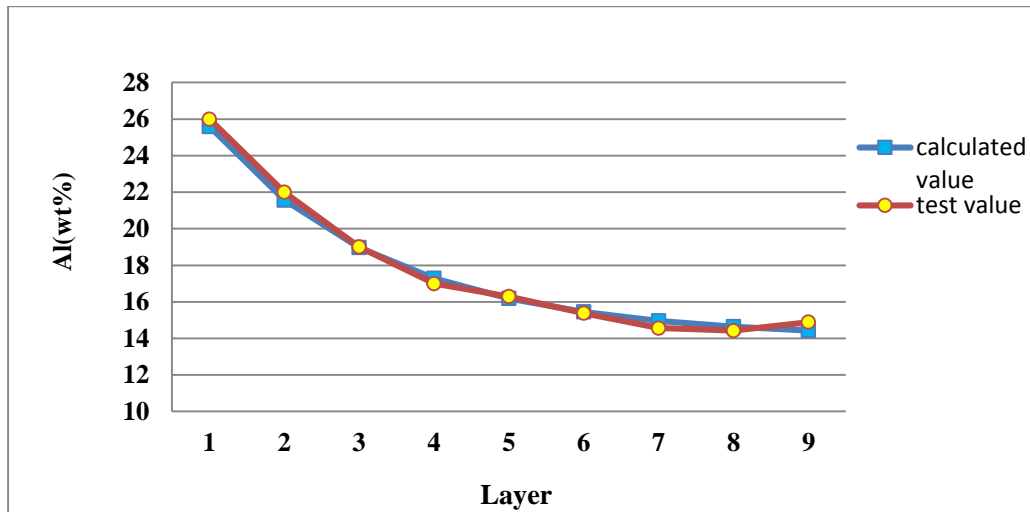


Fig.8 Calculated and measured distributions of element Al

The TiAl alloy underwent several thermal cycles. Rapid heating and cooling result in fine lamellar structures. The temperature history during the fabrication process significantly affected the formation of the lamella structures. The EBSM process employs high power density electron beam and the cooling rate could be as high as $10^3 \sim 10^4$ K/s. The high cooling rate associated with the electron beam melting process is the reason for the formation of fine microstructures in the EBSM products. Peng [13] employed the cyclic heat treatments to obtain fine lamellar microstructures. The grain size could be reduced to $20\mu\text{m}$ after 7 heat treatment cycles. In the rapid heating process, the transformation occurs $\alpha + \gamma \rightarrow \alpha$ when the temperature reaches T_α . The nucleation of fine lamellar microstructure mainly occurs along the grain boundaries and also at the phase interfaces. With the increase of the heating rate, the nuclear rate increases and the transfer rate is faster. In the EBSM process, the formed layers will undergo several rapid heating and cooling cycles.

The microstructure of $\text{Ti}_6\text{Al}_4\text{V}$ and Ti_3Al are the same, consisting of α/α_2 and β . The formation of $\alpha_2\text{-Ti}_3\text{Al}$ is controlled by the content of element Al. Al is an α phase stability element. According to Ti-Al phase diagram of Al, when the content is higher than 7%, $\alpha_2\text{-Ti}_3\text{Al}$ phase will penetrate. Al is α phase stability element, in the first deposition layer of Ti_3Al , the Al element is higher and makes α phase grow up difficult. Also the β stability element is also

high, makes the portion of β phase is higher. That makes the α/α_2 phase become the short acicular shape or the lamellar shape, and their distribution is dispersal too. According to investigate of Yang [6] that the transition zone is the most active diffusion zone, the elements Ti, Al, Cr, Nb and V will diffusion from Ti_3Al side and TiAl side to the diffusion zone, that makes α/α_2 phase accumulation and grow up difficult. The shape of α/α_2 phases become short acicular and the distribution is dispersal.

Conclusion

Titanium dual metal materials were successfully fabricated using EBSM. The effect of fabrication parameters was analyzed in order to understand the composition change and phase transformations. In addition, micro-hardness of transition zone was analyzed. The following conclusions can be derived from this study.

(1)The energy input for Sample-1 is higher than Sample-2 which makes the melting depth larger. According to the composition analysis, the re-melting depth of Sample-1 is 200 μ m, while the re-melting depth in Sample-2 is 80 μ m.

(2)The microstructure of TiAl region was full γ -TiAl and α_2 - Ti_3Al lamellar structure with colony size 15~30 μ m. In the Ti_3Al and Ti6Al4V regions, the microstructures are similar. The microstructure of Ti6Al4V region exhibits prior columnar β grains and α laths forming basket-weave and widmanstetten structure, while in the Ti_3Al part, it consists of short-rod like α_2 phase and β/B_2 phase forming basket-weave structure.

(3) In the transition zone, the micro-hardness shows a normal level distributing in the range of 350-450MPa. The fluctuation is not obvious in the transition zone and the maximum value is up to 450MPa at the top of Ti_3Al alloy.

References

- [1] S.ZGHAL, S.NAKA and A.COURET, A QUANTITATIVE TEM ANALYSIS OF THE LAMELLAR MICROSTURCTURE IN TIAL BASED ALLOY, *ActaMetallurgica*, 1997, 45(7):3005-3015.
- [2]SUN Yan-bo, ZHAO Ye-qing, ZHANG Di, et al, Multilayered Ti-Al intermetallic sheets fabricated by cold rolling and annealing of titanium and aluminum foils, *Trans. Nonferrous Met. Soc. China*, 2011, 21:1722-1727.
- [3]Yuichiro Koizumi, Atsushi Sugihara, Hiroaki Tsuchiya, et al. Selective dissolution of nanolamellar Ti-41 at.% Al alloy single crystals. *ActaMaterialia* 2010,58:2876-2886.
- [4]P.Ravindran,H.Fjellvag, Stabilization of a novel high pressure phase in Ti_3Al .PACS numbers:61.50.Ks
- [5]H.P.XIONG, Q.SHEN, J.G.LI, L.M.ZHANG, Design and microstructures of Ti/TiAl/Al system functionally graded material, *JOURNAL OF MATERIALS SCIENCE LETTERS*, 2000,19 :989-993.

- [6] Yang Hanghang, Yao Zekun, Gao Jun, et al, Influence of Gradient Heat Treatment on Microstructure and Microhardness in Weld Seam of Ti3Al/TC11 Dual Alloys. Rare Metal Material and Engineering, 2010,39(1):0022-0026
- [7]Xie Hang, Zhang Anfeng, Li Dichen, et al, Research on the Cracking of Ti6Al4V-CoCrMo Gradient Material Fabricated by Laser Metal Direct Forming, CHINESE JOURNAL OF LASERS, 2013,40(11):11030031-11030037.
- [8]Xi Mingzhe, Zhang Yongzhong, Tu Yi, et al, 316L STAINLESS STEEL/Ni-BASED ALLOY/Ti6Al4V GRADIENT MATERIALS PREPARED BY LASER RAPID FORMING PROCESS, ACTA METALLURGICA SINICA, 2008,44(7):826-830.
- [9]Xu Zhijun, The microstructures and properties of TC11/ γ -TiAl bio-materials fabricated by laser deposition powders process, Ph.D. Thesis.2013.6
- [10]Douglas C. Hofmann, Scott Roberts, Richard Otis, et al, Developing Gradient Metal Alloys through Radial Deposition Additive Manufacturing, SCIENTIFIC REPORTS, 2014,7:1-8
- [11]Chao Guo, Wenjun Ge, Feng Lin, Dual-Material Electron Beam Selective Melting: Hardware Development and Validation Studies, Engineering 2015,1(1):124-130
- [12]Ohuma I., Fujita Y., Mitsui H., et al. Phase equilibria in the Ti-Al binary system. Acta mater.2000, 48:3113-3123.
- [13]Peng Chaoqun, Huang Baiyun, He Yuehui et al, Microstructural refinement of as-cast TiAl-based alloy by cyclic heat treatment, J.CENT.SOUTH UNIV. TECHNOL,1999,30(1):52-54.